Earth Science Informatics (2024) 17:1907–1921
https://doi.org/10.1007/s12145-023-01218-x

RESEARCH

Suitability of the height above nearest drainage (HAND) model for flood inundation mapping in data-scarce regions: a comparative analysis with hydrodynamic models

Navin Tony Thalakkottukara[1] · Jobin Thomas[1] · Melanie K. Watkins[2] · Benjamin C. Holland[2] · Thomas Oommen[1] · Himanshu Grover[3]

Received: 19 September 2023 / Accepted: 30 December 2023 / Published online: 13 January 2024

Abstract

Unprecedented floods from extreme rainfall events worldwide emphasize the need for flood inundation mapping for floodplain management and risk reduction. Access to flood inundation maps and risk evaluation tools remains challenging in most parts of the world, particularly in rural regions, leading to decreased flood resilience. The use of hydraulic and hydrodynamic models in rural areas has been hindered by excessive data and computational requirements. In this study, we mapped the flood inundation in Huron Creek watershed, Michigan, USA for an extreme rainfall event (1000-year return period) that occurred in 2018 (Father's Day Flood) using the Height Above Nearest Drainage (HAND) model and a synthetic rating curve developed from LIDAR DEM. We compared the flood inundation extent and depth modeled by the HAND with flood inundation characteristics predicted by two hydrodynamic models, viz., HEC-RAS 2D and SMS-SRH 2D. The flood discharge of the event was simulated using the HEC-HMS hydrologic model. Results suggest that, in different channel segments, the HAND model produces different degrees of concurrence in both flood inundation extent and depth when compared to the hydrodynamic models. The differences in flood inundation characteristics produced by the HAND model are primarily due to the uncertainties associated with optimal parameter estimation of the synthetic rating curve. Analyzing the differences between the HAND and hydrodynamic models also highlights the significance of terrain characteristics in model predictions. Based on the comparable predictive capability of the HAND model to map flood inundation areas during extreme rainfall events, we demonstrate the suitability of the HAND-based approach for mitigating flood risk in data-scarce, rural regions.

Keywords Flood inundation mapping · Father's Day Flood · Data-scarce regions · HAND · HEC-RAS 2D · SMS-SRH 2D

Introduction

Flooding is one of the most frequent natural disasters causing significant damage to natural and human resources and affecting millions worldwide. On average, the world witnessed 163 flood events annually between 2001 and 2020 with economic losses worth 34.1 billion US$ (CRED, 2022). However, 2021 recorded a marked increase in flood events (223) and extensive economic losses (74.4 billion US$). While the flood impacts are substantial with the current climate scenario, land use/ land cover conditions, and societal development (Cutter and Emrich 2005; Grahn and Nyberg 2017), climate change and land use/ land cover modifications, particularly urbanization of flood plains, are highly

Communicated by H. Babaie.

✉ Navin Tony Thalakkottukara
navin@go.olemiss.edu

[1] Department of Geology & Geological Engineering, University of Mississippi, Oxford MS-38655, USA

[2] Department of Civil, Environmental, and Geospatial Engineering, Michigan Technological, University, Houghton, MI 49931, USA

[3] Department of Urban Design and Planning, University of Washington, Seattle, WA 98195, USA

likely to escalate flood risks. It is projected to increase the flood risk in a warming climate due to the shifts in precipitation distribution and variability (i.e., intensity, frequency, and duration) by the intensification of the hydrological cycle, as well as changes in socio-economic development factors (Arnell and Gosling 2014; Hirabayashi et al. 2013; Madakumbura et al. 2019; Tellman et al. 2021; Winsemius et al. 2015). Flooding is a leading cause of weather-related natural disasters in the United States, with a Congressional Budget Office estimate of $54 billion in losses (from hurricane winds and storm-related flooding) each year (CBO 2019). According to Swain et al. (2020), the United States is expected to witness a mean increase of ~20% (magnitude) and >200% (frequency) in a 100-year storm event under the high-emission scenario (RCP8.5), yielding a ~30–127% increase in population exposure. Although flood susceptibility across the United States is spatially heterogeneous (Saharia et al. 2017), flood risk significantly differs between urban and rural areas. Predictably much of the research attention focuses on flooding in urban regions overlooking the rural areas, yet those are significantly vulnerable to the impacts of flooding (Bukvic and Harrald 2019; Cutter et al. 2016; Rhubart and Sun 2021).

Along with the different social and physical characteristics (Rhubart and Sun 2021), the decreased flood resilience in rural areas is also a result of the lack (and access) of adequate data and appropriate tools to understand and assess the flood risk. However, the level of flood resilience in rural communities can be enhanced considerably by mapping inundation areas before flood events, as these maps facilitate risk communication to different stakeholders (Henstra et al. 2019). Such non-structural measures help mitigate the impacts of floods and facilitate the development of climate-resilient, risk-informed rural communities. Traditionally, flood inundation mapping uses various hydrodynamic and hydraulic models, such as HEC-RAS, SMS-SRH, MIKE-FLOOD, etc. (Deslauriers and Mahdi 2018; Patel et al. 2017; Vozinaki et al. 2015) which require a variety of basin- and channel-related data input and/or higher computational power and time. However, in most rural regions, such data at finer spatial and temporal scales are unavailable, leaving the rural communities and emergency managers without flood inundation mapping they could use to mitigate flood impacts. Numerous efforts focused on mapping flood hazards without detailed data and observations have resulted in the development of a range of models and tools with different data and computational requirements. For instance, the AutoRoute model has been developed to produce flood inundation maps for extreme flood events from DEM (Follum 2013). Wing et al. (2017) developed a 2D hydrodynamic model, capable of simulating pluvial flooding and fluvial flooding (only in reaches with catchment area exceeding 50 km^2) at ~30 m resolution, for the conterminous US using publicly available data.

In a similar sense, significant research has also been dedicated to simplifying the flood models and their data requirements for universal applications. One such simplified approach is the Height Above the Nearest Drainage (HAND) model (Rennó et al. 2008). The HAND, a DEM-derived terrain attribute, implying the draining potential and soil moisture dynamics, is a suitable descriptor for identifying hydrologically different landscape units (Gharari et al. 2011; Nobre et al. 2011). Major advantages of the HAND-based approach over the hydraulic/hydrodynamic models are the computational efficiency and lower complexity with simplified input data requirements. Numerous researchers have demonstrated the suitability of the HAND model in flood inundation and floodplain mapping studies in various hydroenvironmental conditions (e.g., Bhatt and Srinivasa Rao 2018; Diehl et al. 2021; Rahmati et al. 2018; Scriven et al. 2021; Speckhann et al. 2017) resulting in the application of HAND in different web-based flood inundation mapping as well as real-time and forecast flood guidance systems (e.g., Chaudhuri et al. 2021; Hu and Demir 2021; Johnson et al. 2019; Unnithan et al. 2024; Zheng et al. 2018a).

Since the HAND indicates the difference in the elevation of a given point in the catchment area and the elevation of the stream channel to which the point drains following the flow direction, the inundation depth at the point can be estimated as the difference between the water level (flood stage) and the HAND value. However, the estimation of stage height remains the major constraint, particularly in ungauged watersheds. To overcome this, Zheng et al. (2018b) developed an approach to compute the river channel geometry and estimate the synthetic rating curve (on a reach-average level) based on HAND values. The synthetic rating curve demonstrates the empirical relationship between discharge and stage height for a given reach and its catchment area. Further, Zheng et al. (2018b) noted that optimization of Manning's n generates a reasonable synthetic rating curve comparable to that derived using HEC-RAS and gauge observations. Subsequently, various researchers (e.g., Ghanghas et al. 2022; Johnson et al. 2019; Scriven et al. 2021; Zheng et al. 2022) also tested the performance of the synthetic rating curve at wide spatial scales and recommended it as a viable approach in ungauged basins and data-scarce regions.

Considering the advancements in HAND-based flood inundation mapping, it is also essential to investigate the efficiency and representativeness of the HAND model over data- and computationally-intensive hydraulic/hydrodynamic models. Previous studies comparing the flood inundation extent and depth between HAND and HEC-RAS 2D models suggest that the HAND model generates an

inundation extent similar to that modeled by HEC-RAS 2D. For instance, Afshari et al. (2018) observed that the results of the HAND model are significantly close to the HEC-RAS 2D for flood extent and depth in simple landscapes at large spatial scales. However, significant differences are evident in complex conditions, such as meandering channels and stream confluences. Afshari et al. (2016) reported that the HAND model underestimates inundation extent by up to 40% in a flat, urbanized area with a controlled/managed river channel. In contrast, the model showed improved accuracy in areas having undulating topography. While comparing the flood inundation extent and depth in small headwater catchments of southeastern France, Hocini et al. (2021) reported an overall better performance of hydraulic models (i.e., caRtino 1D, and Floodos 2D) solving Saint-Venant shallow water equations compared to the HAND-based approach.

Since the major limiting factor for developing effective flood mitigation strategies is the lack of reliable data, results of the approaches with less data and computational requirements, such as the HAND model, should be validated with various hydraulic and hydrodynamic models, to assess the applicability of HAND model in rural regions to enhance decision-making for flood risk reduction and adaptation. However, the suitability of the HAND model for flood inundation mapping in data-scarce regions and ungauged watersheds is less explored and assessed. In this study, we assess the relative accuracy of HAND vis-à-vis different hydrodynamic/hydraulic models, viz., HEC-RAS 2D and SMS-SRH 2D, for an extreme magnitude flood event (1000-year return period) in terms of the flood inundation extent and depth in Huron Creek watershed in Michigan, USA.

Father's day flood in Michigan, 2018

The western portion of the Upper Peninsula of Michigan experienced very heavy rainfall on 17 June 2018 with the majority of the rainfall occurring between 2 am and 5 am. The region received 3 to 7 inches (76.2 to 177.8 mm) of rainfall in less than 6 h (NWS, 2018), which the NOAA Precipitation Frequency Atlas (https://hdsc.nws.noaa.gov/hdsc/pfds) described as a 1000-year storm event. Although the storm occurred across the Upper Peninsula, the greatest concentration of the storm centered on Houghton County, resulting in unprecedented widespread flooding across the region known as the Father's Day flood. Hardly any weather events of this severity have occurred in the region, and the flash flooding caused severe damage to residential and public infrastructure worth more than 100 million US$ (WUPPDR 2020). Among the various severely flood-affected areas, the Huron Creek watershed in Houghton is of particular interest because of the enormous damage to infrastructure that occurred along the main channel of Huron Creek. Many culverts and embankments along the main channel displayed evidence of scour, and the culvert at Sharon Avenue failed to cause extended flooding, rerouting the channel bed, and scouring vegetation (Washko 2019). Although the primary source of floodplain mapping information in the region is the Flood Insurance Rate Maps, which are developed by the Federal Emergency Management Agency, the region remains unmapped and therefore lacks flood hazard information (https://msc.fema.gov/portal/home). Hence, in this study, we analyze the suitability of the HAND model to map the flood-prone areas of the Huron Creek watershed by comparing the flooding extent and depth due to the 1000-year storm event produced by the HAND model with HEC-RAS 2D and SMS-SRH 2D simulations and quantify the similarities/differences between the approaches.

Study area: Huron Creek watershed

The Huron Creek watershed is located in the northern part of Houghton County in the Upper Peninsula of Michigan, USA. The watershed drains an area of about 2.8 mi^2 (7.25 km^2) and empties into the Portage Canal, the waterway connected to Lake Superior (Fig. 1). The mainstream of the watershed has a length of about 3.2 mi (5.15 km). The streamflow of Huron Creek is partially regulated by a small dam, Huron Dam, which was built in 1865 to utilize water for mining-related activities, thereby creating Huron Lake. Elevation in the watershed ranges from 1085 to 602 ft (330.7 to 183.5 m). In general, the south and central portions of the watershed are characterized by nearly level to gently sloping surface topography, whereas the north-central part of the watershed is relatively steeper. The average bed slope of Huron Creek upstream of Huron Lake is about 1%, while the average channel bed slope is approximately 4 to 5% between Huron Lake and the Portage Canal (CWS 2009). Although a wide range of soil types occur in the watershed, the predominant soil textures are sand, sandy loam, and gravelly sand (Fig. 2a; Table S1). However, a few soil types, particularly across the southern and northeastern areas of the watershed, have relatively higher fractions of silt content. Among the different land use/ land cover types, forests (38.8%) and wetlands (15.7%) contribute to more than 50% of the catchment area (Fig. 2b). Roughly one-third of the watershed area is developed, and the majority of the urban and built-up lands spread across the downstream areas of the watershed. CWS (2009) reported a drastic increase in the areal extent of the urban and built-up areas in the watershed since 1978 at the cost of forested and agricultural areas as well as rangelands.

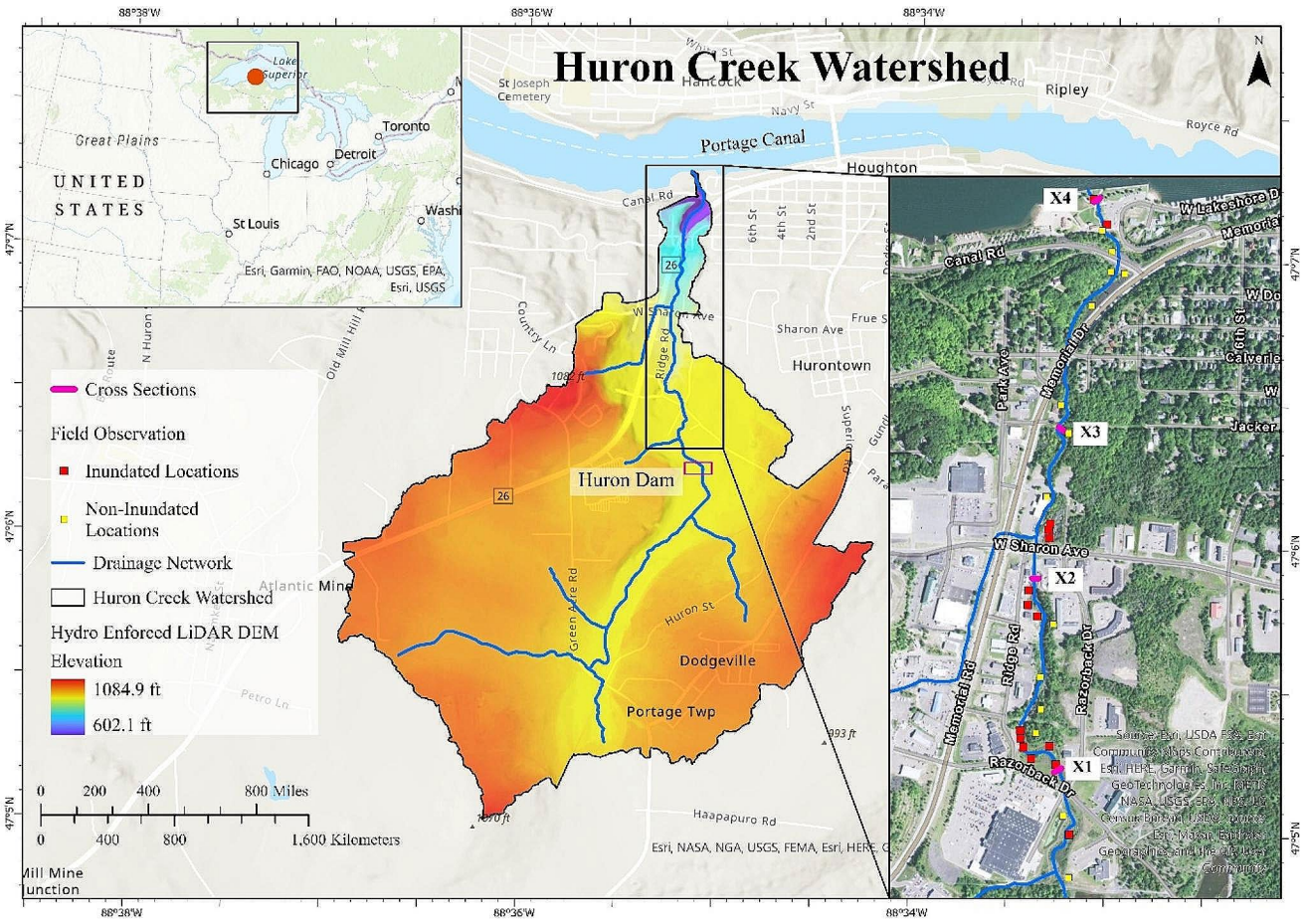

Fig. 1 Study area: Huron Creek watershed (Houghton, Michigan, USA)

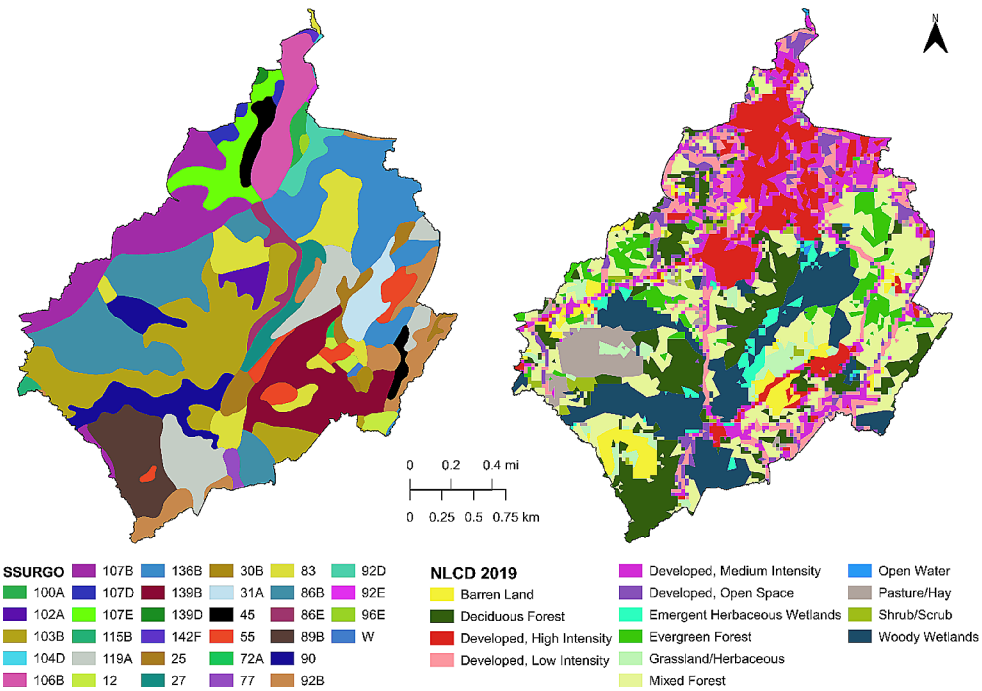

Fig. 2 Spatial distribution of **(a)** soil and **(b)** land use/ land cover types of Huron Creek watershed. Refer to Table S1 (Supplementary Information) for details of the map units

The Huron Creek watershed enjoys a humid continental climate with a warm summer (Koppen Dfb). Based on the climate data records (1952–2012) in the Western Regional Climate Center (https://wrcc.dri.edu), the average minimum temperature during the winter months (December through February) was about 11 °F (-11.67 °C), and the average maximum temperature during summer was approximately 73 °F (22.78 °C). On average, the region receives about 31 inches (787.4 mm) of rainfall annually, with the largest amounts of rainfall in September and January (> 3.0 inches (76.2 mm). The occurrence of extreme rainfall events is infrequent in the climate history of the Huron Creek watershed. However, recent decades witnessed relatively intense storms that caused flooding and bank erosion along Huron Creek. The most recent intense storm event occurred on 17 June 2018 and recorded about 7 inches (177.8 mm) of rainfall in less than 6 h. Some of the other heavy rainfall episodes include the storms that occurred on 4 September 2007 and 16 July 2006, which produced more than 3 inches (76.2 mm) of rainfall in less than 10 h (CWS 2009). The annual average snowfall in the region exceeds 200 inches (5080 mm), predominantly contributed by the lake effect. As a result, snowmelt runoff is a major factor controlling the watershed hydrology of Huron Creek during the spring season. On the other hand, rainfall-derived runoff is significant in the summer and autumn seasons.

Methodology

Simulation of flood discharge using HEC-HMS

We used the HEC-HMS hydrologic model to simulate the Father's Day flood event that occurred in the Huron Creek watershed. The input data for setting up the HEC-HMS model includes the digital elevation model (DEM), land use/ land cover, soil, and rainfall. In this study, we used a LIDAR DEM with a spatial resolution of 2 ft x 2 ft (0.6×0.6 m) for generating the stream network and watershed boundary. The watershed was subdivided into seven sub-watersheds. Land use/ land cover types of the watershed were extracted from the National Land Cover Dataset 2019 (NLCD 2019) (Dewitz & USGS, 2021). We extracted soil data of the watershed from the Soil Survey Geographic Database (SSURGO) (Soil Survey Staff). In this study, we used the Soil Conservation Service Curve Number (SCS-CN) method to estimate the runoff, the SCS unit hydrograph method to transform the runoff volume into a hydrograph, and the Muskingum method for channel routing. We estimated the weighted average curve number of each sub-watershed based on the spatial variability of land use/ land cover types and hydrologic soil groups in the sub-watersheds. The lag time was estimated using the SCS method (Chow et al. 1988), and the routing parameters were computed using the method (for ungauged watersheds) described in USACE (2022). Rainfall data at fine spatial and temporal scales is not available for the watershed and hence, we used the rainfall (at 1-minute intervals) recorded on 17 June 2018 at Keweenaw Research Centre, Michigan Technological University as the meteorological forcing data for the watershed. The Huron Creek watershed does not have an observed hydrograph of the Father's Day flood event. However, the Michigan Department of Environment, Great Lakes and Energy (EGLE) maintains a record of flood discharges of different return periods (up to 500 years). According to the database, the discharge magnitudes corresponding to 100-year and 500-year floods are 440 ft^3/s (12.46 m^3/s) and 650 ft^3/s (18.41 m^3/s) (https://www.egle.state.mi.us/flow/hflowqry.asp). As the EGLE lacks streamflow magnitude for a return period as infrequent as the 0.001% flood, we estimated the 1000-year magnitude on the basis of extrapolation. Hence, we fine-tuned the default parameters of the HEC-HMS model to simulate the flood hydrograph to reasonably match the 1000-year flood discharge magnitude.

HAND

Estimation of the flood inundation depth and extent in the Huron Creek watershed using the HAND model involves three steps: (1) computation of HAND raster for the Huron Creek, (2) derivation of hydraulic properties of the river reach under investigation, and (3) generation of the synthetic rating curve for the reach. Derivation of the HAND model from DEM involves two sets of procedures: (1) generating a seamless, hydrologically-corrected DEM, defining flow paths, and delineating drainage channel network, and (2) deriving the HAND model from the hydrologically-corrected DEM using local drain directions and the drainage network. We used the LIDAR DEM with a spatial resolution of 2 ft x 2 ft (0.6×0.6 m) for computing the HAND raster. First, we identified the hydraulic structures along the stream channel and processed them to create a flow continuum through hydro-enforcing. We used different spatial analyst tools (in ArcGIS) to generate the hydrologically conditioned DEM, flow direction, and flow accumulation. Since the drainage delineation from DEM is sensitive to the channel initiation threshold, we used the USGS National Hydrography Datasets (i.e., NHDPlus flowlines) as the reference for delineating the stream network of the Huron Creek watershed. We calculated the weighted flow accumulation using the channel head source grid cells (from NHDPlus streams) as input and defined the stream raster. Finally, we calculated the HAND using the D∞ flow distance function with the vertical drop option. The computed HAND raster provides

the spatially distributed values of the difference in elevation between a given point (pixel) and the nearest stream (i.e., the downslope grid cell where the flow from the point enters the channel following the local drainage direction). For any given stage height, inundation occurs in pixels with HAND values smaller than the specified stage height. For example, when the water level in a channel reaches 3 ft (0.91 m), the pixels in the floodplain with HAND values less than 3 ft (0.91 m) will be inundated. Thus, the inundation area and average inundation depth for different stage heights were estimated from the HAND raster. These values were used to derive the cross-sectional area (A) and hydraulic radius (R) of the channel reach (see Zheng et al. 2018b for detailed methodology). The reach length and average slope (S) were estimated from the DEM-derived channel network. Although the channel roughness varies along the reach, we used the average value (0.035) of the surveyed reaches in Huron Creek as Manning's n. We used the Manning's equation to generate river discharge at the reach (Eq. 1):

$$Q_i = \frac{1.49}{n} \times A \times R^{\frac{2}{3}} \times S^{\frac{1}{2}} \quad (1)$$

where Q_i is the predicted discharge (in ft^3/s) for any given stage height, *i*. A comprehensive description of the generation of synthetic rating curves using HAND is provided by Zheng et al. (2018b). The river discharges were computed for different stage heights to develop the synthetic rating curve for Huron Creek. The Manning's n for the reach was consistent for all the models. The stage height for the simulated flood discharge by the HEC-HMS model (in Sect. 4.2) was estimated using this synthetic rating curve and the inundation area and depth were estimated from the stage height and HAND raster.

Hydraulic modeling

In this study, we used two hydraulic/hydrodynamic models, viz., HEC-RAS 2D (version 6.3.1) and SMS-SRH 2D for flood inundation mapping in the Huron Creek watershed. HEC-RAS, developed by the Hydrologic Engineering Center (U.S. Army Corps of Engineers), offers capabilities for 1D, 2D, and 1D-2D combined modeling. On the other hand, SMS-SRH 2D is a two-dimensional hydraulic model with a user-friendly graphical interface developed by Aquaveo, featuring a computational engine developed by the Bureau of Reclamation (Aquaveo, 2021; Lai, 2008). We employed a two-dimensional flood routing approach in both models to analyze flooding dynamics. Despite the variations in the model structure, we maintained consistent parameter usage throughout the modeling process. The LiDAR DEM, which was used to derive the HAND model, served as the basis for the terrain model in HEC-RAS 2D and SMS-SRH 2D. Subsequently, we used a computational mesh with a grid size of 10 ft x 10 ft (3×3 m), chosen in consideration of the river channel width and to leverage the high-resolution DEM. Breaklines were strategically placed along the river banks to facilitate water flow through the channel. The hydraulic model domain spanned from downstream of the Huron Dam to the outlet point at the Portage Canal (Fig. 1). Notably, the canal and its backwater effects were omitted from the model, as the canal's stage level remained below that of the stream during the 2018 flood, exerting hardly any influence on the streamflow. Boundary conditions were provided with the simulated hydrograph from the HEC-HMS model as the input, while normal depth was designated as the output condition. Both models relied on the National Land Cover Data Set 2016 (NLCD) as the foundational land use/land cover dataset, with Manning's roughness values assigned based on Chow (1959). Manual adjustments to the land use/land cover data were made where necessary to mitigate the NLCD dataset's coarse spatial resolution (30×30 m). In both models, the unsteady flow module incorporated the Saint Venant equation. Results encompassed flood inundation extent, and inundation depth, which were further analyzed.

Model performance evaluation

Flood inundation maps generated by the three approaches (i.e., HAND, HEC-RAS 2D, and SMS-SRH 2D) were used for the comparative assessment. Each model was simulated for the 1000-year storm event. The inundation extents predicted by the different models were validated using field observations and photographic evidence during the flood event. In this study, we identified 15 locations (from field photographs) that were inundated during the flood and randomly generated 15 locations (within the floodplain) that were not inundated during the flood. Since hardly any data are available on the inundation depth, we did not evaluate the accuracy of the predictions, but the results of the hydraulic/hydrodynamic models were compared against the HAND model to assess the general agreement. The accuracy of the predicted classification was evaluated using different prediction performance measures, such as accuracy, Matthews correlation coefficient (MCC), and F_1 Score (Eqs. 1–5).

$$Accuracy = \frac{(TP + TN)}{(TP + FP + TN + FN)} \quad (1)$$

$$MCC = \frac{(TP * TN) - (FP * FN)}{\sqrt{(TP + FP) * (TP + FN) * (TN + FP) * (TN + FN)}} \quad (2)$$

$$precision = \frac{TP}{(TP + FP)} \quad (3)$$

$$recall = \frac{TP}{(TP + FN)} \tag{4}$$

$$F_1Score = 2 * \frac{precision * recall}{precision + recall} \tag{5}$$

where TP (true positive) and TN (true negative) represent the number of observed data that are correctly classified as inundation and non-inundation, respectively, whereas the false positive (FP) and false negative (FN) are the number of data points that are incorrectly classified. In addition, the area under the receiver operating characteristics curve (ROC-AUC) and precision-recall curve (PRC-AUC) were estimated to assess the overall performance of the model predictions. The overall methodological framework adopted in this study is given in Fig. 3.

Results

Streamflow simulation using HEC-HMS

The catchment area of Huron Creek received about 7 in (177.8 mm) of rainfall in less than 6 h (on 17 June 2018) resulting in significant flooding across the floodplain. The simulated hydrograph of the extreme rainfall event using the HEC-HMS model shows a peak discharge of 808 ft^3/s (22.88 m^3/s) at the outlet of Huron Dam at 4.50 am on 17 Jun 2018 (Fig. 4). Due to the lack of observed data records, the accuracy of the HEC-HMS simulated hydrograph was not assessed. Although the EGLE flood discharge database has the discharge magnitude for floods of different return periods (10, 50, 100, 200, and 500), it does not have streamflow magnitude for a return period as infrequent as a 1000-year flood. The EGLE database indicates that the discharge magnitude corresponding to a 500-year flood is 650 ft^3/s (18.40 m^3/s). Although extrapolation of frequency is not standard hydrological practice, we plotted the flows for the other frequencies on a log probability graph and extended it to the 0.001% frequency. We noted that the HEC-HMS simulated peak flood magnitude of 808 ft^3/s (22.88 m^3/s) for a 1000-year rainfall event is a reasonable estimate when compared to the extrapolated discharge.

Inundation mapping

The flood inundation extent and depth estimated by the HAND, HEC-RAS 2D, and SMS-SRH 2D models were compared for the storm event on 17 June 2018. Since we used the hydrograph at the Huron dam as the inflow boundary condition in the hydraulic/hydrodynamic models, the scope of the comparison is limited to the channel reach between the Huron dam and the outlet point at the Portage Canal (see Fig. 1 for geographic extent). Table 1 facilitates comparison of various metrics of model performance for mapping flood inundation areas in the Huron Creek watershed. The HAND model classified the inundation and non-inundation areas with an accuracy of 80%, slightly lower than that of the hydrodynamic models (i.e., 83%) (Table 1). The non-inundated areas in the watershed were predicted relatively better by all the models than the inundated locations, which is evident in the high values of precision. Further, the HAND model has better precision than the hydraulic/hydrodynamic models (Table 1). On the other hand, while predicting the inundated areas, the hydraulic/hydrodynamic models outperform the HAND model, which is obvious by the recall values. The HAND model has a relatively lower recall (0.60) compared to the HEC-RAS 2D and SMS-SRH 2D models (0.80 and 0.73, respectively) (Table 1). The F1 Scores of the models also show a similar pattern as the score is independent of the number of data that are correctly classified as non-inundated (Chicco and Jurman 2020). The

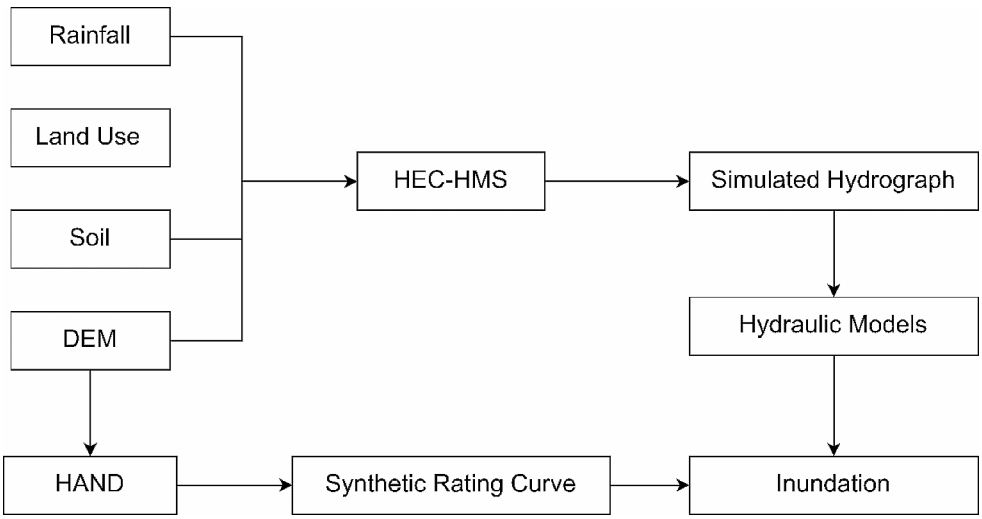

Fig. 3 Methodological framework adopted flood inundation mapping in Huron Creek

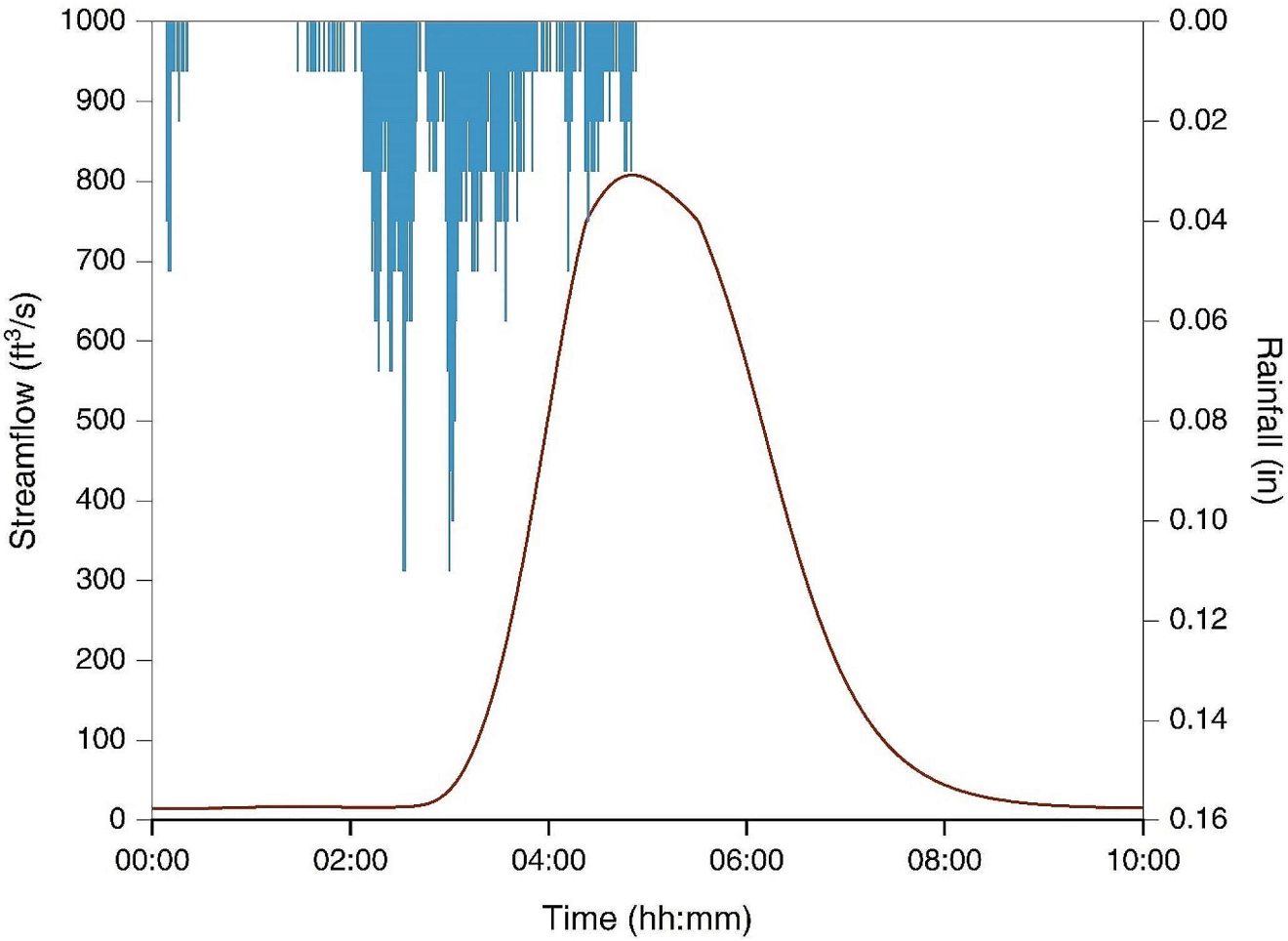

Fig. 4 HEC-HMS simulated flood hydrograph downstream of Huron dam in Huron Creek watershed

Table 1 Model performance measures of inundation extent

	HAND	HEC-RAS 2D	SMS-SRH 2D
Accuracy	0.80	0.83	0.83
MCC	0.65	0.67	0.68
Precision	1.00	0.86	0.92
Recall	0.60	0.80	0.73
F_1-Score	0.75	0.83	0.81
ROC-AUC	0.80	0.83	0.83
PRC-AUC	0.86	0.81	0.84

Table 2 Areal extent of flood inundation modeled by different approaches used in Huron Creek

Channel section	Inundation area (ha)			Mean channel gradient (ft/ft)	Mean valley slope (%)
	HAND	HEC-RAS 2D	SMS-SRH 2D		
Entire reach	2.4	6.1	5.4	0.04	12.6
S1	0.5	0.8	0.7	0.05	13.0
S2	0.3	0.6	0.5	0.02	19.7
S3	0.4	1.1	1.2	0.04	9.0
S4	0.3	2.4	1.7	0.04	11.1

MCC values of all the models are moderate (0.65–0.68) as the coefficient produces a high score only when the models predict good results in all the four categories of the confusion matrix (i.e., TP, TN, FP, and FN), proportional to the size of the inundation and non-inundation datasets (Chicco and Jurman 2020). Although all the models are better at classifying the non-inundated areas, misclassification in the identification of areas under inundation leads to moderate values of MCC. A general comparison of the various performance indicators of different models implies that the HAND model has significant competence in mapping the inundation areas in data-scarce conditions (such as in the Huron Creek watershed) during extreme rainfall events.

A comparison of the inundation extent among the different models indicates that the HAND model resulted in a significantly smaller inundation area compared to the hydraulic models (Table 2). Based on the estimates of the HAND model, the inundation area during the Father's Day flood in the Huron Creek watershed was 2.4 ha, whereas the hydraulic/hydrodynamic models predicted an area more than twice the extent of that of the HAND model. Although

the HAND model underestimates the modeled inundation extent, a similar spatial pattern of inundation extent is noted among the different approaches. Hence, we analyzed the spatial variability of the inundation extent in four channel segments (S1 to S4) of Huron Creek (Fig. 5). The inundation area predicted by the three models in the four channel sections (S1 to S4) shows that the differences between the approaches vary among these sections (Table 2). For instance, the differences in the inundation area between the models are significantly smaller in S1 and S2, whereas S4 has remarkable variability, i.e., 0.3 ha (HAND), 2.4 ha (HEC-RAS 2D), and 1.7 ha (SMS-SRH 2D). Interestingly, the valley slope in S1 and S2 is comparatively higher than in S3 and S4 (Table 2), implying the significance of valley setting in flood inundation estimation using low complexity models, such as HAND.

The flood inundation depths simulated by different models are also compared to assess the general agreement between the models. Since hardly any data on flood inundation depth for the Father's Day flood in Huron Creek is available, we compared the simulated depth generated by the hydraulic/hydrodynamic models against the HAND model. Hence, we limited the scope of the comparative analysis to the intersecting area of the inundation extent produced by the HAND model and the hydrodynamic models. Results indicate that the HAND model underestimated the flood depth in the Huron Creek watershed compared to the HEC-RAS 2D and SMS-SRH 2D simulations (Table 3; Fig. 6). On average, the flood depth produced by the HAND model is about 2 ft (0.6 m) shallower than the HEC-RAS 2D and SMS-SRH 2D simulated depths. Such an underestimation is evident in all the channel segments, except for S1, where the HAND model overestimates flood inundation depth in the upstream and underestimates in the downstream compared to both HEC-RAS 2D and SMS-SRH 2D simulations (Fig. 6). Although S2 (along with S1) shows significant agreement in flood inundation extent between the HAND and the hydraulic/hydrodynamic models (Table 3), the flood

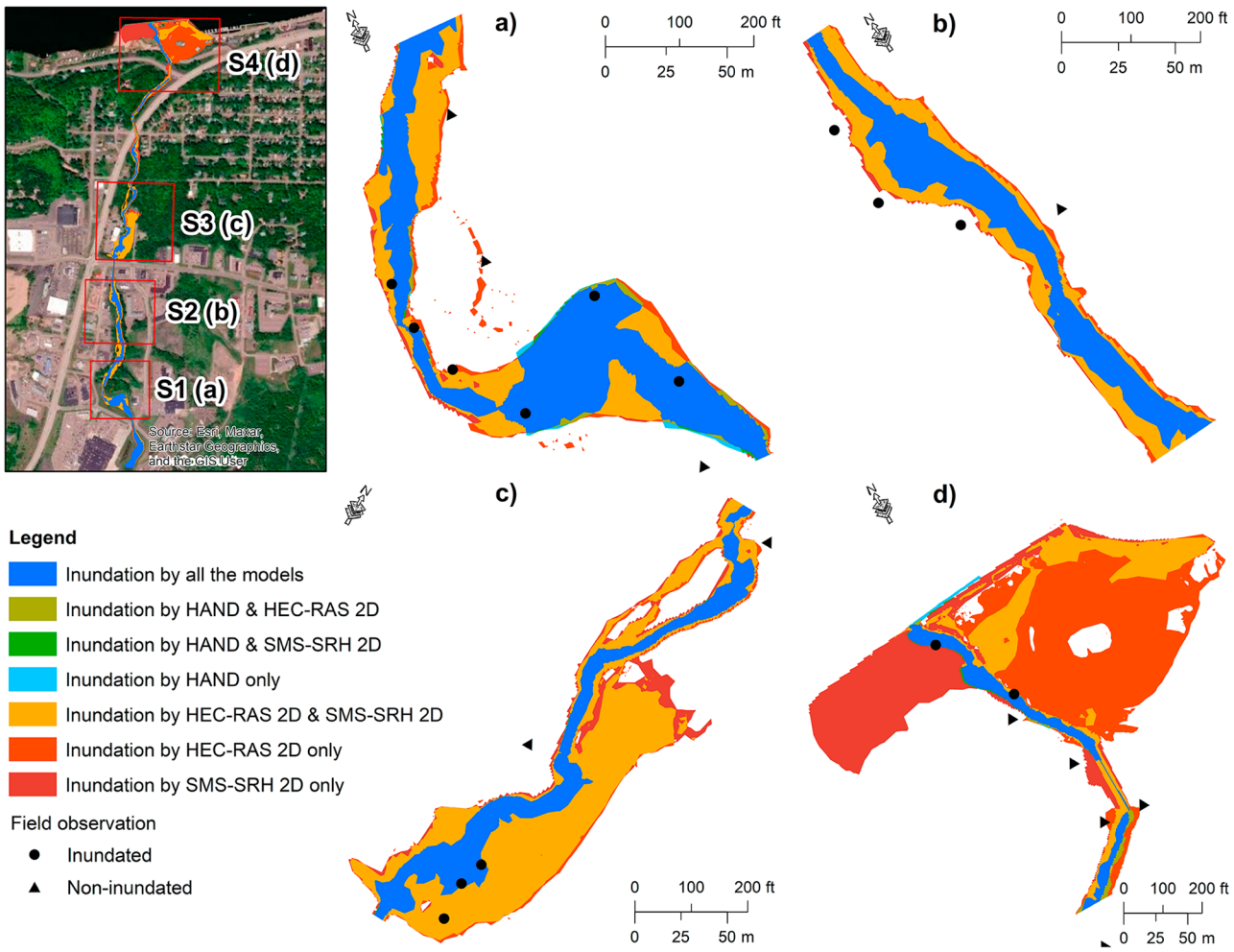

Fig. 5 Inundation extent in the different channel segments (**S1** to **S4**) predicted by HAND, HEC-RAS 2D, and SMS-SRH 2D

Table 3 Difference in flood inundation depth modeled by different approaches used in this study

Channel section	Difference in inundation depth (ft)					
	HAND - HEC-RAS 2D			HAND - SMS-SRH 2D		
	Mean	Minimum	Maximum	Mean	Minimum	Maximum
Entire reach	-1.7	-9.1	3.1	-2.0	-12.9	2.9
S1	0.0	-3.9	3.0	0.2	-3.8	2.9
S2	-2.8	-9.1	-0.1	-2.8	-8.4	0.4
S3	-2.4	-7.9	1.5	-2.3	-7.0	2.0
S4	-1.6	-8.1	3.0	-3.6	-9.5	2.9

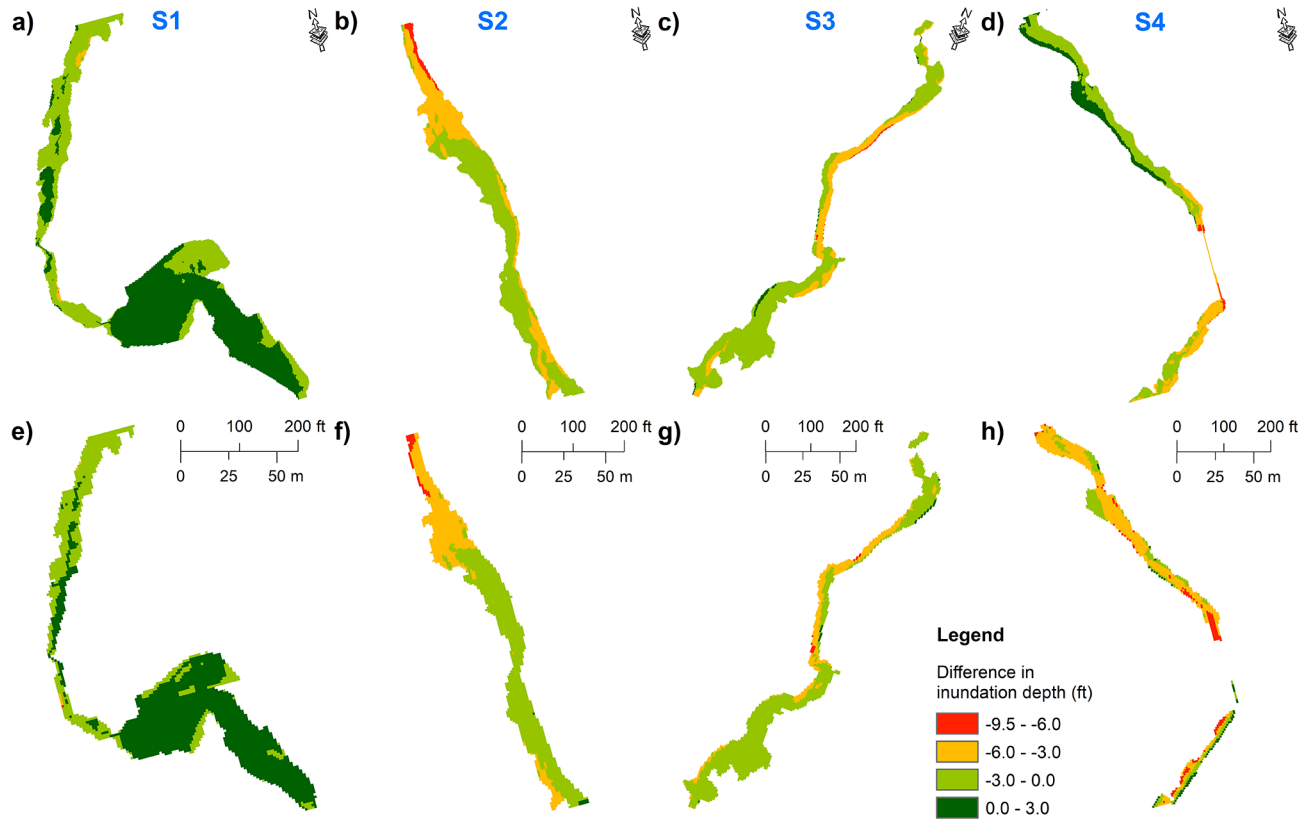

Fig. 6 Differences in the inundation depth predicted by the HAND model in different segments (**S1** to **S4**) compared to HEC-RAS 2D **(a-d)** and SMS-SRH 2D **(e-h)**

depth predicted by the HAND exhibits larger deviation compared to HEC-RAS 2D and SMS-SRH 2D models.

Discussion

The capability of the HAND model to map the inundated areas during the Father's Day flood in the Huron Creek watershed is evident in various model performance measures, except recall (Table 1). A lower recall value (0.60) for the HAND model arises due to misclassifying the areas under inundation as non-inundated areas (i.e., six cases out of 15). Although HEC-RAS 2D (0.80) and SMS-SRH 2D (0.73) also failed to map some of the inundation areas (i.e., three cases in HEC-RAS 2D and four cases in SMS-SRH 2D), the HAND model was less successful than the hydraulic/hydrodynamic models. Interestingly, all three models failed to map inundation at three locations in S2. However, the major cause of the inundation downstream of S2 was the failure of a culvert and associated obstruction. Further, the damaging scour that occurred at S2 modified the downstream fluvial landscape (i.e., S3) by rerouting channel beds, displacing bed load material, and scouring vegetation (Washko 2019). However, the hydraulic/hydrodynamic models accurately predicted the inundation locations in S3, even if the inundation in one of the locations occurred due to the rerouting of the channel at S2. Although it is considered

an accurate prediction, this is a clear case of overestimation of inundation by the hydraulic/hydrodynamic models in S3.

In general, the results of this analysis suggest varying levels of performance of the HAND model compared to the hydraulic/hydrodynamic models, such as HEC-RAS 2D and SMS-SRH 2D, to identify flood inundation areas. The observations of Zheng et al. (2018b) imply that the HAND-based flood inundation mapping shows better performance in hilly, rural catchments where the topographic setting has major control over the flood routing process, compared to urbanized catchments with a gentle slope, where artificial structures significantly affect the hydrodynamic processes. In a similar context, Afshari et al. (2018) observed that the prediction of inundation areas by the HAND model is comparable to the HEC-RAS 2D model in simple fluvial landscapes (e.g., straight, headwater reaches), whereas the HAND model fails in complex conditions, such as meandering sections and tributary confluences. It may be noted that the hydraulic/hydrodynamic model simulations in Huron Creek resulted in significantly larger areas under inundation in general and particularly in S3 and S4 (Table 2; Fig. 5). Similarly, the HEC-RAS 2D simulations of Afshari et al. (2018) also generated wider areas under inundation compared to the outputs generated by low-complexity models, such as HAND and AutoRoute while using simple terrain setup (i.e., without incorporating channel bathymetry or other possible floodplain features, such as levees). However, the predicted depth of inundation by the HAND model along the Huron Creek tends to be underestimated, which could be a reflection of the inability of the model to consider channel hydraulics and hydrodynamics in computing flood inundation. Contrastingly, Afshari et al. (2018) noted that the HAND model overestimates flood inundation depth (compared to HEC-RAS 2D) in simple terrain setup (i.e., without incorporating bathymetry or floodplain features), whereas 'bathymetry-informed' terrain setup results in underestimation of the depth of flood inundation. However, the results of this study show that the HAND model underestimates inundation depth even with a simple terrain setup.

The possibilities of underestimation of the HAND model include (1) a depiction of the actual (bathy-informed) terrain profile in the LIDAR DEM, and (2) uncertainties in the HAND model and the synthetic rating curve. The channel geometry may not be accurately characterized in large rivers even with high-resolution DEMs due to the water column within the channel. Practically, Huron Creek downstream of the Huron Dam is a small stream channel with well-defined valleys and the magnitude of streamflow is low except during intense storm events. Hence, the LIDAR DEM could have captured the actual terrain profile (including bathymetric information) in most of its channel length. However, we did not compare the actual bathymetry and DEM-derived cross-sections to reaffirm this possibility. The uncertainty in the HAND model may be caused by watershed morphological and channel characteristics (Li et al. 2022). The flood inundation estimation using the HAND model heavily relies on the accuracy of the synthetic rating curve generated using the LIDAR DEM. In this study, we used the NHDPlus flowlines to identify the headwater location and Manning's equation to compute the flood discharge. Further, the stage corresponding to the Father's Day flood discharge (808 ft^3/s (22.8 m^3/s) in this case) was estimated from the synthetic rating curve. The inundation depth was calculated by subtracting the HAND raster from the stage height obtained from the rating curve (Zheng et al. 2018b). Hence, the uncertainties in estimating the synthetic rating curve would have significant effects on the flood inundation depth. Although Zheng et al. (2018b) could not generate a globally accurate synthetic rating curve from the HAND raster with a constant Manning's n, they demonstrated that optimizing Manning's n considering the channel roughness condition results in a rating curve comparable to that derived from gauge observations. In this study, we used Manning's n of 0.035 derived from field observations. Further, Washko (2019) also used a similar Manning's n for hydraulic modeling in the Huron Creek watershed. However, the differences in Manning's n along the river reach and the possible range of values were not considered when calculating the synthetic rating curve. Keeping the channel attributes (i.e., cross-sectional area, hydraulic radius, and slope) constant, we independently varied the roughness coefficient, solving for the flood discharge of 808 ft^3/s. In doing so, we noted that that the synthetic rating curve relationships are sensitive to the changes in Manning's n. In addition, terrain and channel characteristics could also affect the accuracy of the rating curve. Godbout et al. (2019) noted that the accuracy of the synthetic rating curve is largely influenced by reach length, reach slope, and hydraulic structures, where short reaches, reaches with low gradients, and reaches close to hydraulic structures were found to predict the poor performance of synthetic rating curve. Similarly, Ghanghas et al. (2022) also showed that channels with low slopes and large catchment areas tend to overpredict the synthetic rating curve, while channels in hilly tracts tend to underpredict.

The HAND model shows similar performance in mapping flooding extent in some sections of Huron Creek (i.e., S1 and S2) compared to the hydraulic/hydrodynamic models. However, large deviations are observed in specific sections (S3 and S4; Table 3) where the valleys are broader than the other sections. This difference could be mostly due to the simplified representation in the HAND model and generalization (i.e., uniform flow, invariant channel roughness). While estimating the synthetic rating curve, the hydraulic properties are averaged assuming uniform channel geometry

along the reach. Although such an assumption could be partly valid for steep channels with uniform morphology in well-defined valleys, the assumption adds to uncertainty in broad valleys. For instance, Hocini et al. (2021) noted large deviations in HAND-based flood inundation estimates compared to hydrodynamic methods in large and flat floodplains, with a longitudinal slope significantly higher than the transverse slope in the floodplain. Flat areas in DEM lack local elevation gradients resulting in an inaccurate representation of local flow direction (Martz and Garbrecht 1998; Tarboton 1997), and hence, inaccurate HAND values thereby erroneous cross-sectional geometry derived from the HAND-based approach. The significant negative bias in the HAND model estimates of flood inundation depth compared to the hydraulic/hydrodynamic models (Table 3) also partly contributed by the generalization of the geometry (Hocini et al. 2021).

The HAND model is sensitive to the channel initiation threshold, one of the major parameters used in HAND-based approaches (Li et al. 2022). In this study, we used the NHD flowlines (mapped at a scale of 1: 24,000) to identify the headwater location. Hence, the difference in the spatial scale between the channel initiation point and the DEM used for HAND estimation also results in discrepancies in hydraulic properties which propagate into the inundation mapping (Garousi-Nejad et al. 2019). Other potential reasons for the deviation between the HAND and hydraulic/hydrodynamic models could be the boundary effects between sub-basins particularly at stream confluences and the absence of representation of backwater effects (Afshari et al. 2018; Hocini et al. 2021). Although many researchers demonstrated the significance of these effects in flood inundation estimates in river channels developed in large floodplains, we noted that such effects are significant in stream channels of smaller rural watersheds too. Considering the limitations of the HAND model for mapping flood inundation, several researchers argued that the HAND model can be improved by proposing various modifications. For example, Godbout et al. (2019) proposed a moving window approach to recalculate the reach slope in Manning's equation as the weighted average over a minimum distance. Similarly, Garousi-Nejad et al. (2019) also suggested various modifications for improving the HAND-based flood inundation mapping, e.g., derivation of hydraulic properties and synthetic rating curves using the DEM-based drainage network and catchments based on evenly spaced nodes along a stream reach, and a hybrid filling-breaching algorithm to hydrologically condition the DEM. It is also suggested to infer stream reach hydraulic roughness using observed past flood inundation data.

Access to flood inundation maps showing potential areas, assets, and populations that are vulnerable is a high priority in the context of flood risk planning and risk reduction programs, particularly in rural regions. The decreased flood resilience in rural regions in the US (e.g., Upper Peninsula in Michigan) is attributed to the lack of data and appropriate tools to assess flood risk calling for the development of flood risk mapping tools for efficient floodplain management (Thomas et al., 2022). Since the HAND is a topography-based model, the approach has several advantages over the traditional hydraulic/hydrodynamic models. The HAND model is conceptually simpler compared to the hydraulic/hydrodynamic models. Further, the applicability of hydraulic/hydrodynamic models has always been hindered by the availability of input data at required spatial and temporal scales and computational requirements. Hence, the HAND-based approach is easy to set up and update and can be useful in ungauged basins to provide quick estimates of potential flood extents and inundation patterns. Despite the varying levels of performance across the different channel segments of Huron Creek, the HAND-based approach reiterates the suitability of the HAND model for flood inundation mapping in data-scarce regions. Hence, flood inundation and risk mapping approaches based on low complexity models, such as HAND have a promising future as these serve as a vital guidance tool for enhancing flood resilience in data-scarce rural regions and ungauged watersheds to a great extent.

Summary and conclusion

This study investigated the suitability of the HAND model for flood inundation mapping in data-scarce regions by comparing the flood inundation characteristics with hydraulic/hydrodynamic models, such as HEC-RAS 2D and SMS-SRH 2D. Flood inundation extent and depth were mapped in the Huron Creek watershed (in Houghton County, Michigan, USA) for an extreme rainfall event (Father's Day flood) with a recurrence interval of more than 1000 years. Being an ungauged watershed, flood discharge for the storm event was simulated using the HEC-HMS model and was used as the input inflow boundary condition of the flood event. The simulated flood hydrograph of the event resulted in a peak discharge of 808 ft^3/s (22.88 m^3/s) at the outlet of Huron Dam. The performance of the various models was assessed using different metrics. A comparison of the performance measures of different models implies the suitability of the HAND model to map the extent of flood inundation areas. While the HAND model slightly underestimates the inundation extent, the hydraulic/hydrodynamic models show overestimation. Further, HEC-RAS 2D shows a relatively larger areal extent compared to SMS-SRH 2D. Among the different channel segments in Huron Creek, S3 and S4, with

less steep valleys, show larger deviations in the inundation area between the HAND and the hydraulic/hydrodynamic models. Further, the HAND model underestimates the flood depth compared to HEC-RAS 2D and SMS-SRH 2D simulations, mostly due to the uncertainties in the estimation of the synthetic rating curve.

Supplementary Information The online version contains supplementary material available at https://doi.org/10.1007/s12145-023-01218-x.

Acknowledgements The authors thank the Western Upper Peninsula Planning Development Region for facilitating data collection.

Author contributions Conceptualization: Navin Tony Thalakkottukara, Jobin Thomas, Benjamin C. Holland, Thomas Oommen, Melanie K. Watkins, Himanshu Grover. Methodology: Navin Tony Thalakkottukara, Jobin Thomas, Benjamin C. Holland, Thomas Oommen, Melanie K. Watkins, Himanshu Grover. Formal analysis and investigation: Navin Tony Thalakkottukara, Jobin Thomas, Melanie K. Watkins, Benjamin C. Holland. Writing - original draft preparation: Jobin Thomas, Navin Tony Thalakkottukara. Writing - review and editing: Thomas Oommen, Melanie K. Watkins. Visualization: Navin Tony Thalakkottukara, Jobin Thomas. Funding acquisition: Thomas Oommen, Himanshu Grover. Supervision: Thomas Oommen, Himanshu Grover. All authors reviewed the manuscript.

Funding The authors would like to acknowledge the financial support from the US National Science Foundation grant (Award No 2133279) to conduct this research.

Data availability The datasets generated during and/or analyzed during the current study are available from the corresponding author on request.

Declarations

Competing interests The authors declare that there are no financial or personal interests that could be construed as competing with the presented research.

References

Afshari S, Omranian E, Feng D, Rajib A, Tavakoly A, Snow A, Cohen S, Merwade V, Fekete B, Sharif H, Beighley E (2016) Comparison of physical and semi-empirical hydraulic models for Flood inundation mapping. AGU Fall Meeting, San Francisco

Afshari S, Tavakoly AA, Rajib MA, Zheng X, Follum ML, Omranian E, Fekete BM (2018) Comparison of new generation low-complexity Flood inundation mapping tools with a hydrodynamic model. J Hydrol 556:539–556. https://doi.org/10.1016/j.jhydrol.2017.11.036

Aquaveo (2021) SMS 13.0: the complete surface-water solution. https://www.aquaveo.com/software/sms-surface-water-modeling-system-introduction

Arnell NW, Gosling SN (2014) The impacts of climate change on river Flood risk at the global scale. Clim Change 134(3):387–401. https://doi.org/10.1007/s10584-014-1084-5

Bhatt CM, Srinivasa Rao G (2018) HAND (height above nearest drainage) tool and satellite-based geospatial analysis of Hyderabad (India) urban Floods, September 2016. Arab J Geosci 11(19). https://doi.org/10.1007/s12517-018-3952-1

Bukvic A, Harrald J (2019) Rural versus urban perspective on coastal flooding: the insights from the U.S. Mid-atlantic communities. Clim Risk Manage 23:7–18. https://doi.org/10.1016/j.crm.2018.10.004

CBO (2019) *Expected costs of damage from hurricane winds and storm-related flooding*. https://www.cbo.gov/publication/55019

Chaudhuri C, Gray A, Robertson C (2021) InundatEd-v1.0: a height above nearest drainage (HAND)-based Flood risk modeling system using a discrete global grid system. Geosci Model Dev 14(6):3295–3315. https://doi.org/10.5194/gmd-14-3295-2021

Chicco D, Jurman G (2020) The advantages of the Matthews correlation coefficient (MCC) over F1 score and accuracy in binary classification evaluation. BMC Genomics 21(1):6. https://doi.org/10.1186/s12864-019-6413-7

Chow VT, Maidment DR, Larry W (1988) Applied Hydrology. McGraw-Hill Inc

CRED. (2022) *2021 disasters in numbers*. https://cred.be/sites/default/files/2021_EMDAT_report.pdf

Cutter SL, Emrich C (2005) Are natural hazards and Disaster losses in the U.S. increasing? Eos Trans Am Geophys Union 86(41). https://doi.org/10.1029/2005eo410001

Cutter SL, Ash KD, Emrich CT (2016) Urban-rural differences in Disaster Resilience. Annals of the American Association of Geographers 106(6):1236–1252. https://doi.org/10.1080/24694452.2016.1194740

CWS (2009) *Huron Creek watershed management plan*. https://pages.mtu.edu/~asmayer/HuronCreek/HuronCreek.htm

Deslauriers S, Mahdi T-F (2018) Flood modelling improvement using automatic calibration of two dimensional river software SRH-2D. Nat Hazards 91(2):697–715. https://doi.org/10.1007/s11069-017-3150-6

Dewitz J (2021) & USGS. *National Land Cover Database (NLCD) 2019 Products (ver. 2.0, June 2021)* Version 2.0). https://doi.org/10.5066/P9KZCM54

Diehl RM, Gourevitch JD, Drago S, Wemple BC (2021) Improving Flood hazard datasets using a low-complexity, probabilistic floodplain mapping approach. PLoS ONE 16(3):e0248683. https://doi.org/10.1371/journal.pone.0248683

Follum ML (2013) *AutoRoute rapid flood inundation model*

Garousi-Nejad I, Tarboton DG, Aboutalebi M, Torres-Rua AF (2019) Terrain Analysis Enhancements to the Height Above Nearest Drainage Flood Inundation Mapping Method. Water Resour Res 55(10):7983–8009. https://doi.org/10.1029/2019wr024837

Ghanghas A, Dey S, Merwade V (2022) Evaluating the reliability of synthetic rating curves for continental scale Flood mapping. J Hydrol 606. https://doi.org/10.1016/j.jhydrol.2022.127470

Gharari S, Hrachowitz M, Fenicia F, Savenije HHG (2011) Hydrological landscape classification: investigating the performance of HAND based landscape classifications in a central European

meso-scale catchment. Hydrol Earth Syst Sci 15(11):3275–3291. https://doi.org/10.5194/hess-15-3275-2011

Godbout L, Zheng JY, Dey S, Eyelade D, Maidment D, Passalacqua P (2019) Error Assessment for Height above the nearest drainage inundation mapping. JAWRA J Am Water Resour Association 55(4):952–963. https://doi.org/10.1111/1752-1688.12783

Grahn T, Nyberg L (2017) Assessment of pluvial Flood exposure and vulnerability of residential areas. Int J Disaster Risk Reduct 21:367–375. https://doi.org/10.1016/j.ijdrr.2017.01.016

Henstra D, Minano A, Thistlethwaite J (2019) Communicating Disaster risk? An evaluation of the availability and quality of Flood maps. Nat Hazards Earth Syst Sci 19(1):313–323. https://doi.org/10.5194/nhess-19-313-2019

Hirabayashi Y, Mahendran R, Koirala S, Konoshima L, Yamazaki D, Watanabe S, Kim H, Kanae S (2013) Global Flood risk under climate change. Nat Clim Change 3(9):816–821. https://doi.org/10.1038/nclimate1911

Hocini N, Payrastre O, Bourgin F, Gaume E, Davy P, Lague D, Poinsignon L, Pons F (2021) Performance of automated methods for flash Flood inundation mapping: a comparison of a digital terrain model (DTM) filling and two hydrodynamic methods. Hydrol Earth Syst Sci 25:2979–2995. https://doi.org/10.5194/hess-2020-597

Hu A, Demir I (2021) Real-Time Flood Mapping on client-side web systems using HAND model. Hydrology 8(2). https://doi.org/10.3390/hydrology8020065

Johnson JM, Munasinghe D, Eyelade D, Cohen S (2019) An integrated evaluation of the National Water Model (NWM)–Height above nearest drainage (HAND) Flood mapping methodology. Nat Hazards Earth Syst Sci 19(11):2405–2420. https://doi.org/10.5194/nhess-19-2405-2019

Lai Y (2008) SRH-2D version 2: theory and user's manual. U.S. Department of the Interior-Bureau of Reclamation. https://www.usbr.gov/tsc/techreferences/computer%20software/models/srh2d/index.html

Li Z, Mount J, Demir I (2022) Accounting for uncertainty in real-time Flood inundation mapping using HAND model: Iowa case study. Nat Hazards 112(1):977–1004. https://doi.org/10.1007/s11069-022-05215-z

Madakumbura GD, Kim H, Utsumi N, Shiogama H, Fischer EM, Seland O, Scinocca JF, Mitchell DM, Hirabayashi Y, Oki T (2019) Event-to-event intensification of the hydrologic cycle from 1.5 degrees C to a 2 degrees C warmer world. Sci Rep 9(1):3483. https://doi.org/10.1038/s41598-019-39936-2

Martz LW, Garbrecht J (1998) The treatment of flat areas and depressions in automated drainage analysis of raster digital elevation models. Hydrol Process 12(6):843–855. https://doi.org/10.1002/(sici)1099-1085(199805)12:6%3C843::Aid-hyp658%3E3.0.Co;2-r

Nobre AD, Cuartas LA, Hodnett M, Rennó CD, Rodrigues G, Silveira A, Waterloo M, Saleska S (2011) Height above the nearest drainage – a hydrologically relevant new terrain model. J Hydrol 404(1–2):13–29. https://doi.org/10.1016/j.jhydrol.2011.03.051

NWS. (2018) *2018 Father's Day weekend: Upper Michigan flooding*. National Weather Service, National Oceanic and Atmospheric Administration. Retrieved 01-24-2023 from https://www.weather.gov/mqt/fathersday2018weekendflooding

Patel DP, Ramirez JA, Srivastava PK, Bray M, Han D (2017) Assessment of Flood inundation mapping of Surat city by coupled 1D/2D hydrodynamic modeling: a case application of the new HEC-RAS 5. Nat Hazards 89(1):93–130. https://doi.org/10.1007/s11069-017-2956-6

Rahmati O, Kornejady A, Samadi M, Nobre AD, Melesse AM (2018) Development of an automated GIS tool for reproducing the HAND terrain model. Environ Model Softw 102:1–12. https://doi.org/10.1016/j.envsoft.2018.01.004

Rennó CD, Nobre AD, Cuartas LA, Soares JV, Hodnett MG, Tomasella J, Waterloo MJ (2008) HAND, a new terrain descriptor using SRTM-DEM: mapping terra-firme rainforest environments in Amazonia. Remote Sens Environ 112(9):3469–3481. https://doi.org/10.1016/j.rse.2008.03.018

Rhubart D, Sun Y (2021) The social correlates of Flood risk: variation along the US rural–urban continuum. Popul Environ 43(2):232–256. https://doi.org/10.1007/s11111-021-00388-4

Saharia M, Kirstetter P-E, Vergara H, Gourley JJ, Hong Y (2017) Characterization of Floods in the United States. J Hydrol 548:524–535. https://doi.org/10.1016/j.jhydrol.2017.03.010

Scriven BWG, McGrath H, Stefanakis E (2021) GIS derived synthetic rating curves and HAND model to support on-the-fly Flood mapping. Nat Hazards 109(2):1629–1653. https://doi.org/10.1007/s11069-021-04892-6

Speckhann GA, Chaffe B, Goerl PLF, Abreu R, J. J. d., Flores A, J. A (2017) Flood hazard mapping in Southern Brazil: a combination of flow frequency analysis and the HAND model. Hydrol Sci J 63(1):87–100. https://doi.org/10.1080/02626667.2017.1409896

Swain DL, Wing OEJ, Bates PD, Done JM, Johnson KA, Cameron DR (2020) Increased Flood exposure due to Climate Change and Population Growth in the United States. Earths Future 8(11). https://doi.org/10.1029/2020ef001778

Tarboton DG (1997) A new method for the determination of flow directions and upslope areas in grid digital elevation models. Water Resour Res 33(2):309–319. https://doi.org/10.1029/96wr03137

Tellman B, Sullivan JA, Kuhn C, Kettner AJ, Doyle CS, Brakenridge GR, Erickson TA, Slayback DA (2021) Satellite imaging reveals increased proportion of population exposed to Floods. Nature 596(7870):80–86. https://doi.org/10.1038/s41586-021-03695-w

Thomas J, Mohan S, Thalakkottukara NT, Oommen T, Watkins MK, Grover H, Williams R, Meadows G (2022) Development of a flood risk modeling system for enhanced resilience of rural regions. In: AGU fall meeting 2022. Chicago, 12-16 December, 2022.

Unnithan SLK, Biswal B, Rüdiger C, Dubey AK (2024) A novel conceptual Flood inundation model for large scale data-scarce regions. Environ Model Softw 171. https://doi.org/10.1016/j.envsoft.2023.105863

USACE (2022) HEC-HMS Technical Reference Manual. CPD-74B. https://www.hec.usace.army.mil/confluence/hmsdocs/hmstrm

Vozinaki A-EK, Karatzas GP, Sibetheros IA, Varouchakis EA (2015) An agricultural flash Flood loss estimation methodology: the case study of the Koiliaris basin (Greece), February 2003 Flood. Nat Hazards 79(2):899–920. https://doi.org/10.1007/s11069-015-1882-8

Washko S (2019) Flood inundation mapping for Huron Creek, Houghton County, Michigan. Michigan Technological University]. Houghton

Wing OEJ, Bates PD, Sampson CC, Smith AM, Johnson KA, Erickson TA (2017) Validation of a 30 m resolution Flood hazard model of the conterminous United States. Water Resour Res 53(9):7968–7986. https://doi.org/10.1002/2017wr020917

Winsemius HC, Aerts JCJH, van Beek LPH, Bierkens MFP, Bouwman A, Jongman B, Kwadijk JCJ, Ligtvoet W, Lucas PL, van Vuuren DP, Ward PJ (2015) Global drivers of future river Flood risk. Nat Clim Change 6(4):381–385. https://doi.org/10.1038/nclimate2893

WUPPDR (2020) Houghton county: 2020–2025 hazard mitigation plan. W. U. P. P. D. Region. https://www.cityofhoughton.com/wp-content/uploads/2020/07/HoughtonCountyHazardMitigationPlan.pdf

Zheng X, Maidment DR, Tarboton DG, Liu YY, Passalacqua P (2018a) GeoFlood: large-Scale Flood Inundation Mapping based on High-Resolution Terrain Analysis. Water Resour Res 54(12). https://doi.org/10.1029/2018wr023457

Zheng X, Tarboton DG, Maidment DR, Liu YY, Passalacqua P (2018b) River Channel Geometry and rating curve estimation using height above the nearest drainage. JAWRA J Am Water Resour Association 54(4):785–806. https://doi.org/10.1111/1752-1688.12661

Zheng X, D'Angelo C, Maidment DR, Passalacqua P (2022) Application of a large-scale terrain-analysis-based Flood Mapping System to Hurricane Harvey. JAWRA J Am Water Resour Association 58(2):149–163. https://doi.org/10.1111/1752-1688.12987